



The 8.2 ka cooling event caused by Laurentide ice saddle collapse



I.S.O. Matero*, L.J. Gregoire, R.F. Ivanovic, J.C. Tindall, A.M. Haywood

University of Leeds, School of Earth and Environment, Woodhouse Lane, Leeds, LS2 9JT, UK

ARTICLE INFO

Article history:

Received 8 December 2016
Received in revised form 28 May 2017
Accepted 3 June 2017
Available online xxxx
Editor: M. Frank

Keywords:

8.2 ka event
Laurentide ice sheet
ice saddle collapse
abrupt climate change
Paleoclimate
Atlantic Meridional Overturning Circulation

ABSTRACT

The 8.2 ka event was a period of abrupt cooling of 1–3 °C across large parts of the Northern Hemisphere, which lasted for about 160 yr. The original hypothesis for the cause of this event has been the outburst of the proglacial Lakes Agassiz and Ojibway. These drained into the Labrador Sea in ~0.5–5 yr and slowed the Atlantic Meridional Overturning Circulation, thus cooling the North Atlantic region. However, climate models have not been able to reproduce the duration and magnitude of the cooling with this forcing without including additional centennial-length freshwater forcings, such as rerouting of continental runoff and ice sheet melt in combination with the lake release. Here, we show that instead of being caused by the lake outburst, the event could have been caused by accelerated melt from the collapsing ice saddle that linked domes over Hudson Bay in North America. We forced a General Circulation Model with time varying meltwater pulses (100–300 yr) that match observed sea level change, designed to represent the Hudson Bay ice saddle collapse. A 100 yr long pulse with a peak of 0.6 Sv produces a cooling in central Greenland that matches the 160 yr duration and 3 °C amplitude of the event recorded in ice cores. The simulation also reproduces the cooling pattern, amplitude and duration recorded in European Lake and North Atlantic sediment records. Such abrupt acceleration in ice melt would have been caused by surface melt feedbacks and marine ice sheet instability. These new realistic forcing scenarios provide a means to reconcile longstanding mismatches between proxy data and models, allowing for a better understanding of both the sensitivity of the climate models and processes and feedbacks in motion during the disintegration of continental ice sheets.

© 2017 The Authors. Published by Elsevier B.V. This is an open access article under the CC BY license (<http://creativecommons.org/licenses/by/4.0/>).

1. Introduction

Around 8,200 yr ago, there was an abrupt cooling of 1–3 °C across large parts of the Northern Hemisphere which lasted around 160 yr (Barber et al., 1999; Thomas et al., 2007; Morrill et al., 2013a). The event has been described as the ‘Goldilocks abrupt climate change event’ for testing ocean response to climate change in coupled ocean–atmosphere models (Schmidt and LeGrande, 2005). This is because: (i) the climate change is well constrained with well dated, widespread data (Morrill et al., 2013a); (ii) its duration and amplitude (~1–3 °C change in Europe) (Veski et al., 2004; Feurdean et al., 2008) are relevant to the timescale and magnitude of future climate change; (iii) and most crucially, the forcing of the event is thought to be well understood, robust and quantifiable. As such, it is an ideal candidate for multi-model comparisons and evaluations.

The original hypothesis for the cause of the event was that the proglacial Lakes Agassiz and Ojibway catastrophically drained into the Labrador Sea following the collapse of an ice dam over

Hudson Bay. This freshened the North Atlantic, leading to a weakening of the Atlantic Meridional Overturning Circulation (AMOC), which reduced the northward meridional heat transport and resulted in cooling of the Northern Hemisphere. However, simulating this lake discharge in climate models (typically by including a 1 yr freshwater flux of 2.5 Sv) causes a climate perturbation that recovers in a matter of decades (LeGrande and Schmidt, 2008; Tindall and Valdes, 2011; Morrill et al., 2013b), whereas the cold anomaly seen in climate proxy records lasts 160–400 yr (Rohling and Pälike, 2005; Ellison et al., 2006; Thomas et al., 2007; Morrill et al., 2013a).

Recent studies have suggested that the lake outburst was not the sole forcing of the 8.2 ka event, but instead that additional freshwater fluxes (FWF) have been integral in causing the climate perturbation (Clark et al., 2001; Meissner and Clark, 2006; Carlson et al., 2009a, 2009b; Gregoire et al., 2012; Wagner et al., 2013). Sediment core data indicates that freshwater input through Hudson Strait increased by at least 0.13 ± 0.03 Sv for several centuries around the timing of the event (Carlson et al., 2009b), the freshwater likely originating from the opening of a new drainage pathway for continental runoff (Clark et al., 2001; Meissner and Clark, 2006) and accelerated melt of the Laurentide

* Corresponding author.

E-mail address: eeisom@leeds.ac.uk (I.S.O. Matero).

Ice Sheet (Carlson et al., 2008; Gregoire et al., 2012). Energy mass balance and ice sheet modelling studies also suggest that the collapse of an ice saddle connecting the Labrador and Baffin domes over Hudson Bay released significant amounts of freshwater over several hundred years (Carlson et al., 2008, 2009a; Gregoire et al., 2012).

The volume of the freshwater stored in the lake prior to the release was equivalent to 0.22 to 0.96 m of Global Mean Sea Level Rise (GMSLR) (Leverington et al., 2002; Törnqvist and Hijma, 2012). This water was likely released in several pulses (Teller et al., 2002), and a meltwater pulse corresponding to ~ 0.23 m GMSLR over 0.5–5 yr has commonly been used for examining the effects of the lake drainage, the volume based on hydraulic modelling of the lake flood (Clarke et al., 2004). This was a substantial increase in meltwater discharge over a short period, but relatively small in comparison to estimated early Holocene GMSLR: 3.0 ± 1.2 m from 8.54 to 8.20 ka (Törnqvist and Hijma, 2012), 1.5 ± 0.7 m from 8.3 to 8.2 ka (Li et al., 2012) and ~ 4.5 m from 8.2 to 7.6 ka (Lambeck et al., 2014). Around 2.0 m to 3.9 m of the sea level rise over 8.2 to 7.6 ka has been attributed to the remnant Laurentide Ice Sheet (LIS) after the separation of ice domes over Hudson Bay (Ullman et al., 2016). Any Antarctic contribution to the GMSLR was small compared to the LIS in the early Holocene, approximately ~ 2.5 –3 cm per century from 10 to 8 ka (Briggs and Tarasov, 2013).

Climate modelling studies have shown that while the lake release alone is not sufficient to simulate the 8.2 ka cooling event in its full duration, the addition of other sources of freshwater can maintain the cooling for 100–200 yr (e.g. Renssen et al., 2001; Wiersma et al., 2006; Meissner and Clark, 2006; LeGrande and Schmidt, 2008; Wiersma and Jongma, 2010). Several of these studies investigated the climatic response to a lake release and an additional FWF of 0.172 Sv, either representing a background flux from the ice sheet for 400–900 yr (e.g. Wiersma et al., 2006; Wiersma and Jongma, 2010) or a rerouting of the continental runoff for 500 yr following the lake flood (Meissner and Clark, 2006). These background or rerouted fluxes likely overestimated the amount of FWF entering the oceans, as the GMSLR contribution of 0.172 Sv would have been ~ 1.6 m per century. The rate is similar to the estimated GMSLR between 8.3 and 8.2 ka (Li et al., 2012), but more than the estimated sea level rise over longer time periods around the timing of the event (Törnqvist and Hijma, 2012; Lambeck et al., 2014). The recovery of ocean circulation strength following freshwater forcings to North Atlantic has been found to be highly model-dependent (Stouffer et al., 2006), and it is possible that the Earth System Models of Intermediate Complexity (EMIC) used in the studies mentioned above require a larger than realistic perturbation to reproduce the cooling interpreted from the records. Recently, Wagner et al. (2013) using CCSM3 (Community Climate System Model Version 3) found good agreement between their simulations and the proxy records when using a more moderate FWF. They included a background flux of 0.05 Sv prior to the Lake Agassiz flood and a freshwater flux of ~ 0.13 Sv for 100 yr (from Carlson et al., 2009b) following the flood. The source of freshwater for the latter period was assumed to be the melting of ice over Hudson Bay (Wagner et al., 2013). The timing and magnitude of a combination of forcings from multiple sources are hard to constrain, which could make the use of the 8.2 ka event for benchmarking climate models difficult.

The disintegration of the LIS is thought to have accelerated at the start of the Holocene (~ 9 –7 ka) when strongly negative mass balance, driven by the combination of orbital changes and high greenhouse gas concentrations (Gregoire et al., 2015), triggered a surface mass balance feedback, leading to the collapse of the ice saddle over Hudson Bay (Carlson et al., 2008, 2009a; Gregoire et al., 2012, 2015). The ice-sheet modelling study by Gregoire et al. (2012) suggested that the LIS would have released ~ 5.5 m GM-

SLR equivalent over 400 yr, as an ice saddle connecting the domes around Hudson Bay collapsed. This is a compelling mechanism, not least because the rate of saddle collapse meltwater release from LIS is similar to the estimated GMSLR for the period leading to the 8.2 ka event (~ 15 m ka $^{-1}$, Lambeck et al., 2014), highlighting the large contribution of the LIS to the increase in global mean sea level in the early Holocene. The melting of the ice saddle could have been further intensified both in amplitude and duration as mechanisms of marine ice sheet instability (Dyke and Prest, 1987) and interactions of the ice sheet and Lake Agassiz have not yet been included in ice sheet modelling studies of this event.

Here, for the first time, we simulate the climatic effects of a meltwater pulse produced by the Hudson Bay ice saddle collapse by using meltwater scenarios that are constrained by both plausible melt rates based on known processes of ice retreat (Gregoire et al., 2012) and plausible melt volumes derived from sea level records (Törnqvist and Hijma, 2012; Lambeck et al., 2014). Our five transient meltwater scenarios (Table 1) simulated by the HadCM3 coupled atmosphere–ocean–vegetation General Circulation Model (GCM) evaluate the ice saddle collapse as the sole forcing of the event in comparison to lake discharge forcing.

2. Methods

2.1. Model description

We use the HadCM3 fully coupled atmosphere–ocean–vegetation GCM developed by the UK Met Office (Valdes et al., 2017; MOSES2.1 and using the TRIFFID dynamical vegetation model). The atmosphere component of the model has a horizontal resolution of $2.5^\circ \times 3.75^\circ$, with 19 unevenly spaced vertical layers. The ocean component has a horizontal resolution of $1.25^\circ \times 1.25^\circ$ with 20 unevenly spaced vertical levels, and maximum vertical resolution in the upper 300 m, with a rigid lid. Physical parameterisations in the ocean include eddy-mixing and thermodynamic sea–ice schemes.

2.2. Experiment design

Our experiments start from an earlier spin-up simulation by Singarayer et al. (2011), which was run for 2000 yr. For this spin-up simulation, the model was setup to match 9 ka conditions, including updating the ice sheets and associated boundary conditions (ice-sheet mask, topography, river routing, land–sea mask, bathymetry, which all follow the ICE-5G reconstruction by Peltier, 2004), orbital parameters and atmospheric trace gases (265 ppmv CO₂, 666 ppbv for CH₄, 259 ppbv for N₂O). These were applied as anomalies from the preindustrial; see Singarayer et al. (2011) for details and references therein. These boundary conditions are kept constant throughout all the subsequent simulations in order to examine the effects of the freshwater forcing. The end of the spin-up was used to initialise a *control* simulation with a fixed freshwater flux of 0.05 Sv and an ensemble of simulations with time-varying freshwater fluxes (Table 1).

The ocean component of the model has a rigid lid, and hydrological fluxes such as river runoff and evaporation are therefore represented as virtual salinity fluxes. In our simulations the freshwater from the ice sheet is introduced by decreasing the salinity of oceanic grid boxes at the surface over a region of the Labrador Sea (45 – 70° N, 50 – 70° W). We defined the area of freshwater release to encompass the western coast and most of the Labrador Sea south of 70° N, using a large enough area to allow the rigid lid model to accommodate the resulting decrease in salinity. The outflow of freshwater from the Hudson Strait has been suggested to have exited the Labrador Sea as a more coastally confined southward

Table 1

Freshwater input to the Labrador Sea in our simulations. The forcing in the time-varying experiments increases linearly from the control forcing (0.05 Sv) to the peak value at model year 200, followed by a decrease back to the background forcing resulting in a triangular shape for the freshwater pulse representing the ice saddle collapse (Fig. 1c). The equivalent sea level rise is based on the volume of the total freshwater input over 400 yr.

Simulation name	Forcing strength (Sv)	Forcing length (yr)	Saddle collapse volume (m ³)	Equivalent total sea level rise (m)
Control	0.05	–	–	1.77
Lake_2yr	0.05 & 1.30	2	–	1.99
4.24m_300yr	0.05–0.24	300	8.83×10^{14}	4.24
4.24m_200yr	0.05–0.33	200	8.83×10^{14}	4.24
4.24m_100yr	0.05–0.61	100	8.83×10^{14}	4.24
3.62m_200yr	0.05–0.26	200	6.62×10^{14}	3.62
3.62m_100yr	0.05–0.47	100	6.62×10^{14}	3.62

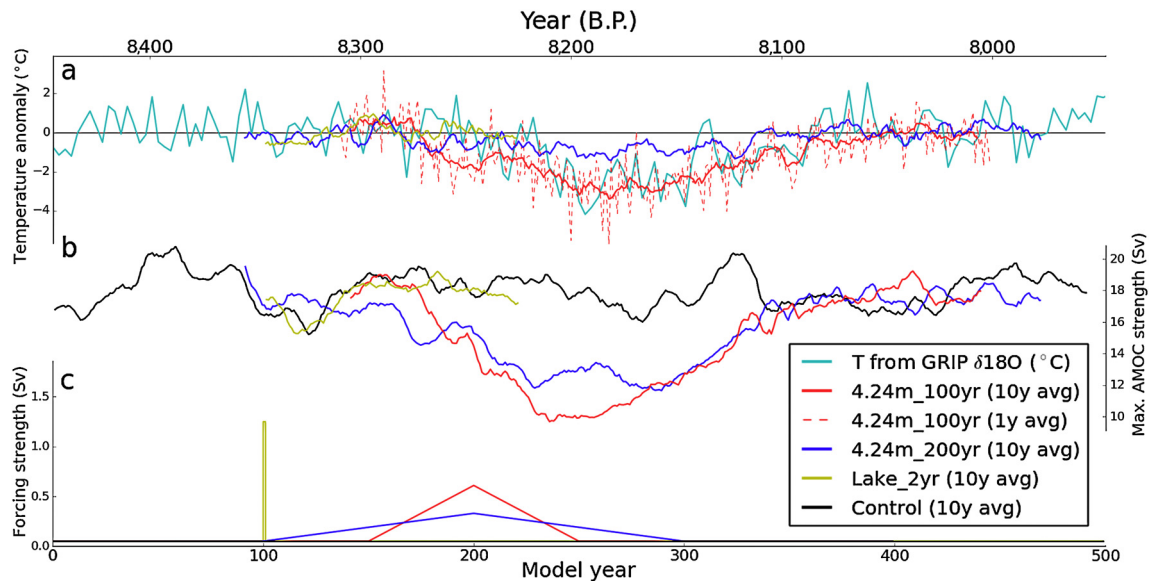


Fig. 1. Time series of (a) the surface air temperature over central Greenland (69–76°N, 36–43°W) in the 4.24m_100yr, 4.24m_200yr and *Lake_2yr* simulations; (solid lines are 10-yr running means, red, dark blue and yellow respectively) and one year running mean of the 4.24m_100yr simulation (red dashed line), compared to the GRIP temperature reconstruction from ice core $\delta^{18}\text{O}$ (Thomas et al., 2007) (light blue); (b) the 10 yr running mean maximum strength of the Atlantic Meridional Overturning Circulation (AMOC) in the 4.24m_100yr (red), 4.24m_200yr (dark blue), *control* (black) and *lake_2yr* (yellow); (c) the freshwater forcing flux in the model experiments (same colours as b). (For interpretation of the references to colour in this figure legend, the reader is referred to the web version of this article.)

flow, supported by both proxy evidence (Hoffman et al., 2012; Lewis et al., 2012) and a high-resolution ocean–ice circulation model (Condron and Winsor, 2011). As a result of using a large hosing area, the modelled freshening pattern in the Labrador Sea is potentially too extensive regionally.

The background flux of 0.05 Sv in the *control* simulation is based on a numerical reconstruction of the estimate of the long-term discharge through the St. Lawrence River from the deglaciation of the Laurentide ice sheet (Licciardi et al., 1999). The freshwater fluxes in the saddle collapse simulations are input on top of the background flux, and run for a total of 500 yr with three lengths for the saddle collapse: 100, 200 and 300 yr (Fig. 1c). The forcing increases linearly from the background meltwater flux to the peak value at model year 200, followed by a linear decrease back to the control value. The volume of the freshwater input in the ice sheet meltwater pulse simulations is equivalent to GMSLR of 3.6 and 4.2 m over 400 yr, of which 1.77 m is due to the background flux. For comparison, we also ran a lake release simulation (2 yr pulse of 1.25 Sv), consistent with simulations of the lake outburst (Clarke et al., 2004).

2.3. Model-data comparison

We compare the temperature signal of the 8.2 ka event in geological records and in our experiment at locations of individual proxy records (Morrill et al., 2013a) (Figs. 2 and 3). The duration

and mean deviation of the event in simulations 4.24m_100yr and 4.24m_200yr are shown in Fig. 3, and a more thorough data-model comparison including the signal in other simulations is shown in Table 2. The event is defined as ongoing when the temperatures in the simulation are outside the 2-sigma variability range in the *control* run, following the method used for identifying anomalous events from the variability of the background climate state for the proxy record compilation (Morrill et al., 2013a). Both the *control* run and the simulations have been detrended using linear regression and smoothed by a 30-yr running mean to be more representative of the sampling frequency of the geological records. The duration of the climate anomalies for the temperature proxies (Morrill et al., 2013a) were identified using a two-tailed z-test method, whereas we define the event duration as the longest continuous period when the modelled temperatures are outside the 2-sigma variability of the *control*. The surface air temperatures (comparison with terrestrial records) and sea surface temperatures (comparison with marine records) are averaged over areas centred at the sites of the records (2 × 2 grid boxes for terrestrial locations, 3 × 3 grid boxes for marine locations and 2 × 3 grid boxes for the GRIP location; Table 2). The modelled surface air temperatures are from the height of 2 m above the surface, and the sea surface temperatures are volume-weighted means calculated from the top 164 m (8 model levels). This was chosen to represent the varying depths at which the key foraminifera that are used as proxies for sea surface temperature are most abundant, as for example

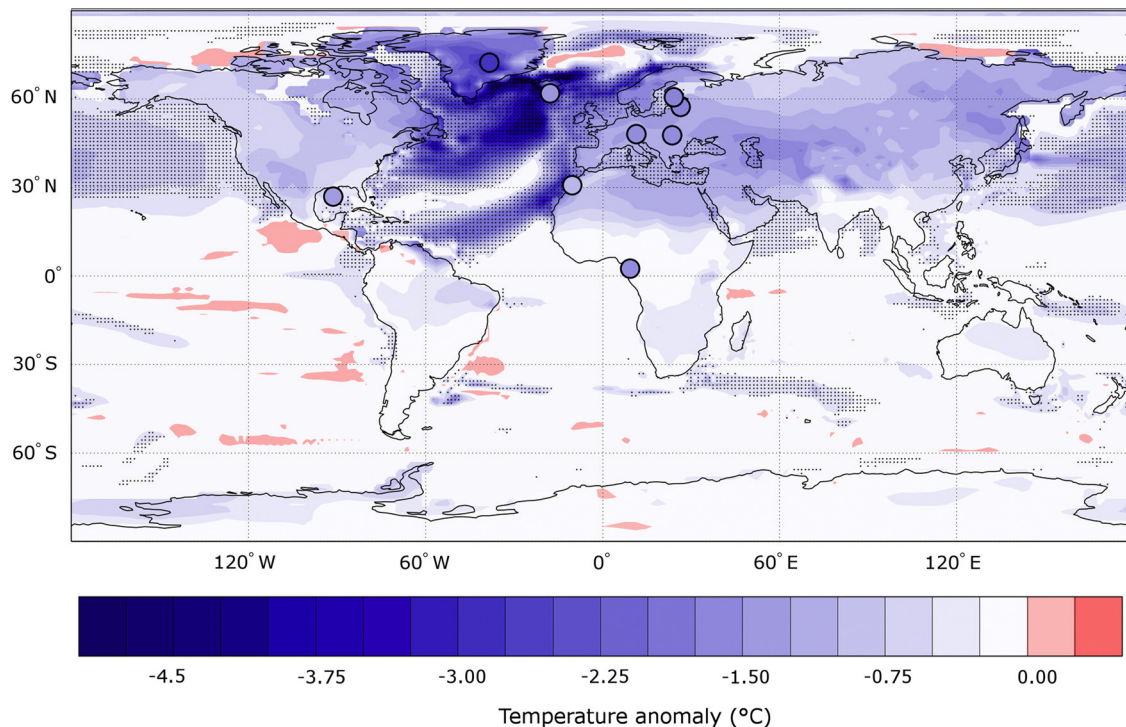


Fig. 2. Maximum annual surface temperature change in the 100 yr long meltwater pulse experiment (4.24m_100yr minus control) using a 50-yr running mean. The upper ocean temperature (top 164 m) is shown for marine regions and surface air temperature is shown over continents. The overlain filled circles show geological reconstructions (Morrill et al., 2013a) of surface air temperature and upper ocean mean temperature anomalies associated with the 8.2 ka event, with numbering referring to the sites in Fig. 3.

Neogloboquadrina pachyderma (left-coiling) has shown abundance maxima between the surface and 175 m (Mortyn and Charles, 2003). Model level 8 (113–164 m) also represents the thermocline depth at the RAPID-12-1k site, where the simulated annual mean mixed layer depth is ~125–150 m following the saddle collapse.

3. Results

3.1. Temperature response

The freshwater scenarios all produce a freshening of the North Atlantic, particularly along the modern subtropical gyre and in the Greenland, Iceland and Norwegian Seas (Fig. 4a), in a pattern that broadly matches freshwater spread from Hudson Strait in a high-resolution ocean model (Condon and Winsor, 2011). The 100 and 200 yr-long meltwater pulse simulations (4.24m_100yr and 4.24m_200yr, respectively; Fig. 1) agree in both the magnitude and duration of climate change compared to the comprehensive compilation of 8.2 ka event data (Morrill et al., 2013a) (Fig. 2, 3; Table 2). In particular, there is a striking agreement in Greenland surface air temperature evolution between the 4.24m_100yr simulation and the temperature reconstruction from the GRIP and GISP2 ice cores (Fig. 1a; Thomas et al., 2007; Kobashi et al., 2007), which are some of the records that provide the most accurate constraints on the amplitude and temporal evolution of the event. Furthermore, the scale of the annual variability in the modelled surface air temperatures (red dashed line in Fig. 1a) matches the decadal-scale variability seen in the GRIP ice core record.

Previously, this multi-decadal variability led to the widely adopted paradigm that the 8.2 ka event occurred in two phases, with a 69 yr central event superimposed on a 160 yr cooling period (Rohling and Pälike, 2005; Thomas et al., 2007). Based on this, Gregoire et al. (2012) proposed that the shorter central event was caused by a proglacial lake outburst mid-way through the saddle

collapse meltwater pulse (e.g. by removing or weakening the ice dam thought to have walled-in the lake), and that the saddle collapse was responsible for the centennial-scale cooling. Here, we find that a 100 yr-long meltwater pulse is capable of producing a climate signal that matches the Greenland record through time (Fig. 1a), without the need for further freshwater forcing (such as the lake release). In addition, a simulated lake release with 1.25 Sv of freshwater over 2 yr produces no distinct temperature anomaly over central Greenland (yellow line in Fig. 1a). Based on these results, we propose that the two-phase event inferred from proxy records is in fact the signal of multi-decadal variability superimposed on a ~150 yr cooling, caused by the meltwater from Hudson Bay saddle collapse entering the Labrador Sea through the Hudson Strait. The climatic response to the freshwater flux from the saddle collapse could have been further amplified if a significant fraction of the FWF discharge was in the form of icebergs (Wiersma and Jongma, 2010). Crucially, our simulations suggest that there is no need for a lake outburst event, or any other additional forcing to explain the 8.2 ka event; it may simply have been a product of ice sheet instability, mass balance feedbacks and change in river routing.

The climate proxy records compared with the model results in Figs. 2–3 and Table 2 were selected because they meet all of the following criteria (from Morrill et al., 2013a): (i) they record annual temperatures, (ii) they have detected the 8.2 ka climate anomaly, (iii) they have high enough temporal resolution to allow for a meaningful comparison to climate model output. In addition to the excellent match with the GRIP ice core record, the spatial pattern of modelled mean temperature changes in the 4.24m_100yr simulation is in agreement with the signal of the 8.2 ka event inferred from terrestrial climate proxy records from Europe (sites 2–5 in Fig. 3; Table 2). As shown in Fig. 2, most of the Northern Hemisphere undergoes a 0.5–1.5 °C cooling in the 4.24m_100yr simulation, which is within the uncertainty range of available palaeoclimate data, indicative of mean cooling of 1–1.6 °C

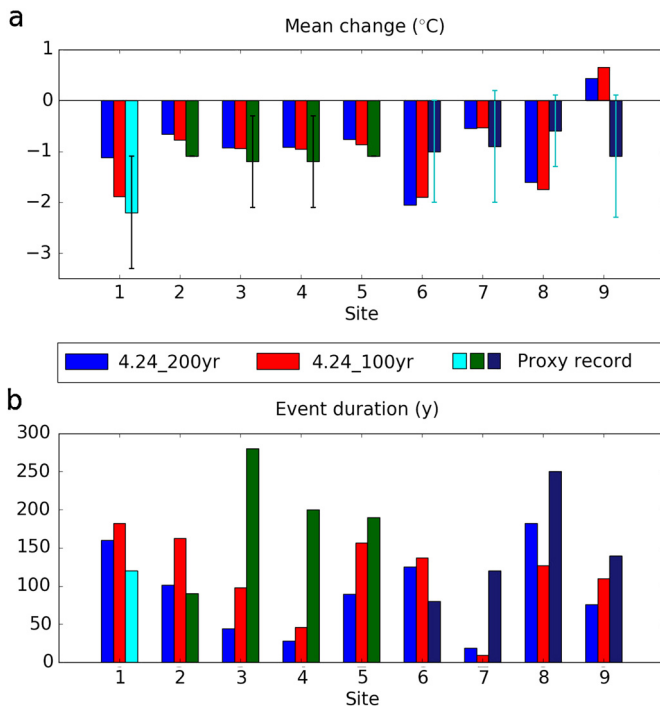


Fig. 3. Comparison of modelled and reconstructed (Morrill et al., 2013a) mean surface temperature change at sites with detected quantitative annual temperature anomalies of the 8.2 ka event, shown in terms of (a) amplitude (°C) and (b) duration (yr) of temperature change (°C). The simulated mean change and duration are calculated from the 30-yr running mean. The event has been defined as ongoing when the simulated temperature values are outside the 2-sigma variability range of the control simulation. Temperature proxy records are indicated in light blue for ice cores, green for terrestrial and dark blue for marine. Estimated errors for individual temperature proxy records, as reported by original investigators (Morrill et al., 2013a), are shown in black and grey in panel a. Locations of the temperature proxy records are shown in Fig. 2 and averaging areas in Table 2. (For interpretation of the references to colour in this figure legend, the reader is referred to the web version of this article.)

over the European continent during the event (Fig. 2; Grafenstein et al., 1998; Veski et al., 2004; Sarmaja-Korjonen and Seppä, 2007; Feurdean et al., 2008). It is worth noting that the marine and terrestrial temperatures inferred from proxy records contain large uncertainty; with errors of 0.7 and 1.2 °C respectively; a magnitude similar to the signal (see discussion in Morrill et al., 2013a). In the ocean model, we observe the most pronounced cooling in the northern North Atlantic, the Labrador Sea, the southern Greenland–Iceland–Norwegian seas, and along the south-westward reaching track of the subtropical gyre (Fig. 2). The 4.24m_100yr and 4.24m_200yr simulations reproduce a cooling pattern that is indicative of changes similar to the changes reconstructed from marine proxy records (LoDico et al., 2006; Kim et al., 2007; Weldeab et al., 2007; Thornalley et al., 2009), except for the Gulf of Mexico (Fig. 3, site 7), where the simulated cooling is too small and too short. The model could either have inadequate sensitivity in this region, or be missing feedback processes that amplify the initial cooling and extend the duration. At a few other marine sites, the same simulations produce a larger cooling than Mg/Ca proxy records (sites 6 and 8) or produce a slight warming instead of a cooling (site 9). This mismatch could indicate that sea surface temperature in HadCM3 is overly sensitive to North Atlantic freshening or that oceanic processes such as upwelling are not being properly represented at individual proxy record sites (e.g. sites 8 and 9). Alternatively, the cooling reconstructed from proxy records might have been dampened by environmental and biotic processes such as migration of planktons in the water column. Finally, some of the changes observed in the marine proxies might not be a

result of the 8.2 ka event as the age models of the proxies can contain substantial uncertainty due to reservoir effects. We conclude that the general good agreement of the proxy records and the simulations in both duration and magnitude further supports the hypothesis that the saddle collapse mechanism was responsible for causing the event.

3.2. AMOC response and precipitation response

Shoaling of the mixed layer depth north of 60°N (Fig. 4e) is indicative of reduced deep water formation, which leads to a 55% decrease in the maximum strength of the AMOC from 17.9 ± 1.5 Sv (Fig. 1b) in the control simulation, down to 8.0 Sv in 4.24m_100yr. Atlantic Meridional Overturning Circulation strength remains in this subdued state (outside the 1σ variability range of the control run) for ~ 150 yr in both the 4.24m_100 yr and 4.24m_200yr simulations (Fig. 1b). Comparison with proxy data is challenging, as quantitative records of the AMOC strength in the early Holocene are not available, but qualitative records suggest that the flow speeds of two major modern branches of the Atlantic Deepwater, the Denmark Strait Overflow Water (DSOW) and the Iceland Scotland Overflow Water (ISOW), were diminished for 100 yr (Kleiven et al., 2008; DSOW) and 400 yr (Ellison et al., 2006; ISOW). The estimated reduction in the DSOW flow speed between ~ 8.38 and 8.27 ka is coeval with a ~ 100 to 200 yr minimum in the ISOW flow speed commencing at ~ 8.29 ka (Ellison et al., 2006). Together these studies suggest that the integrated export of North Atlantic Deepwater from the Nordic Seas was at a minimum centred around 8.29 ka, with a temporal offset between the minimum NADW flow speeds between the two locations, and that the total export of NADW was diminished for ~ 400 yr from 8.49 ka onwards (Ellison et al., 2006). Since the 100 and 200 yr pulses produce similar AMOC anomalies, our results support the suggestion by Wagner et al. (2013), that the volume of the freshwater released has a stronger influence on ocean circulation than the duration of the pulses, when operating at these centennial scales of ice saddle collapse. The sensitivity of the AMOC to freshwater perturbations varies between GCMs (Stouffer et al., 2006), and future work should address testing the response of the climate and ocean circulation to freshwater forcing of saddle collapse scenarios using different GCMs. Furthermore, robustly reconstructing the duration and magnitude of North American ice sheet melt would allow for using the 8.2 ka event for benchmarking and constraining the models used to simulate future climate change.

The pattern of precipitation anomalies resulting from the saddle collapse is consistent in all our simulations, and mainly varies in magnitude with larger and shorter meltwater pulses producing larger precipitation changes. Here we discuss the changes in the 4.24m_100yr simulation (Fig. 4c). The most pronounced large-scale change is simulated at the Atlantic tropics, where the precipitation North of the equator undergoes a significant decrease (up to 50%), and precipitation south of the equator increases by 40–60%. This dipole change supports the idea that the mean position of the Intertropical Convergence Zone shifted southward as a result of increased freshwater flux to the North Atlantic, as has been inferred from precipitation proxy records by e.g. Morrill et al. (2013a). The precipitation changes outside the tropical latitudes are mostly not significant according to Welch's t test at 99% level, apart from the increase in precipitation in the Barents Sea, an area for which no robust precipitation proxy records are not available. Another notable feature is that precipitation has been suggested to have increased in Scandinavia based on geological records from Sweden and Norway (Morrill et al., 2013a), but our simulations in fact indicate non-significantly drier conditions in the region.

Table 2

The 8.2 ka event as captured by quantitative temperature proxies (Morrill et al., 2013a), compared to the 30 yr moving averages of modelled sea surface temperatures and surface air temperatures at individual sites of geological records (Grafenstein et al., 1998; Veski et al., 2004; LoDico et al., 2006; Kim et al., 2007; Sarmaja-Korjonen and Seppä, 2007; Weldeab et al., 2007; Feurdean et al., 2008; Thornalley et al., 2009). Top 8 vertical levels (164 m) were used to represent the sea surface for the marine sites apart from South Iceland Rise, for which the model level corresponding to depths of 113–164 m was used (3 × 3 grid boxes were used for marine locations, 2 × 2 grid boxes for terrestrial locations apart for GISP2, for which 3 × 2 grid boxes are used to centre the box at the ice core location). The event is defined as ongoing when the temperature values are outside the 2-sigma variability of the detrended control run (see methods).

30 yr moving average		4.24m_200yr		Duration	4.24m_100yr		Duration	Proxy		Duration	Proxy	Model	Record
Location	Max	Mean	(yr)	Max	Mean	(yr)	Max	Mean	(yr)	location	area	type	
	(°C)	(°C)		(°C)	(°C)		(°C)	(°C)					
GISP2	−1.74	−1.12	160	−2.97	−1.89	182	−3.3	−2.20	120	72.5°N, 38.5°W	69–76°N, 36–43°W	Terrestrial	
Ammersee, Germany	−0.88	−0.66	101	−1.38	−0.78	163	−1.3	−1.10	90	48.1°N, 11.5°E	46–51°N, 9–17°E	Terrestrial	
Lake Rõuge, Estonia	−0.65	−0.93	44	−1.34	−0.94	98	−2.6	−1.20	280	57.4°N, 26.5°E	56–61°N, 24–32°E	Terrestrial	
Lake Arapisto, Finland	−1.05	−0.92	28	−1.16	−0.96	46	−2.2	−1.20	200	60.6°N, 24.1°E	59–64°N, 21–28°E	Terrestrial	
Stereogiu, Romania	−0.96	−0.76	89	−1.42	−0.87	157	−1.6	−1.10	190	47.8°N, 23.6°E	46–51°N, 21–28°E	Terrestrial	
South Iceland Rise (thermocline)	−3.12	−2.05	125	−3.12	−1.90	137	−1.2	−1.00	80	62.1°N, 17.8°W	60–64°N, 16–19°W	Marine	
Gulf of Mexico	−0.42	−0.55	19	−0.62	−0.53	9	−1.3	−0.90	120	27.0°N, 91.4°W	25–29°N, 89–93°W	Marine	
Cape Ghir (surface)	−2.25	−1.61	182	−2.5	−1.75	127	−0.7	−0.60	250	30.8°N, 10.3°W	29–33°N, 8–12°W	Marine	
Gulf of Guinea	0.69	0.44	76	1.25	0.65	110	−1.9	−1.10	140	2.5°N, 9.4°E	0–4°N, 8–12°E	Marine	

30 yr moving average		4.24m_300yr		Duration	3.62m_200yr		Duration	3.62m_100yr		Duration	Proxy	Model	Record
Location	Max	Mean	(yr)	Max	Mean	(yr)	Max	Mean	(yr)	location	area	type	
	(°C)	(°C)		(°C)	(°C)		(°C)	(°C)					
GISP2	−1.60	−1.16	149	−1.08	−0.92	46	−1.50	−1.19	96	72.5°N, 38.5°W	69–76°N, 36–43°W	Terrestrial	
Ammersee, Germany	−0.86	−0.56	134	−0.51	−0.44	34	−0.97	−0.64	67	48.1°N, 11.5°E	46–51°N, 9–17°E	Terrestrial	
Lake Rõuge, Estonia	−0.77	−0.70	12	–	–	0	−0.94	−0.81	37	57.4°N, 26.5°E	56–61°N, 24–32°E	Terrestrial	
Lake Arapisto, Finland	–	–	0	–	–	0	−0.99	−0.83	24	60.6°N, 24.1°E	59–64°N, 21–28°E	Terrestrial	
Stereogiu, Romania	−1.04	−0.69	83	−0.65	−0.55	19	−1.29	−0.86	81	47.8°N, 23.6°E	46–51°N, 21–28°E	Terrestrial	
South Iceland Rise (thermocline)	−1.90	−1.43	162	−1.90	−1.46	90	−1.90	−1.43	97	62.1°N, 17.8°W	60–64°N, 16–19°W	Marine	
Gulf of Mexico	−0.67	−0.56	9	0.54	0.44	12	−0.85	−0.70	12	27.0°N, 91.4°W	25–29°N, 89–93°W	Marine	
Cape Ghir (surface)	−2.10	−1.52	225	−1.92	−1.50	129	−2.39	−1.72	92	30.8°N, 10.3°W	29–33°N, 8–12°W	Marine	
Gulf of Guinea	0.32	0.23	16	0.48	0.33	47	0.89	0.59	69	2.5°N, 9.4°E	0–4°N, 8–12°E	Marine	

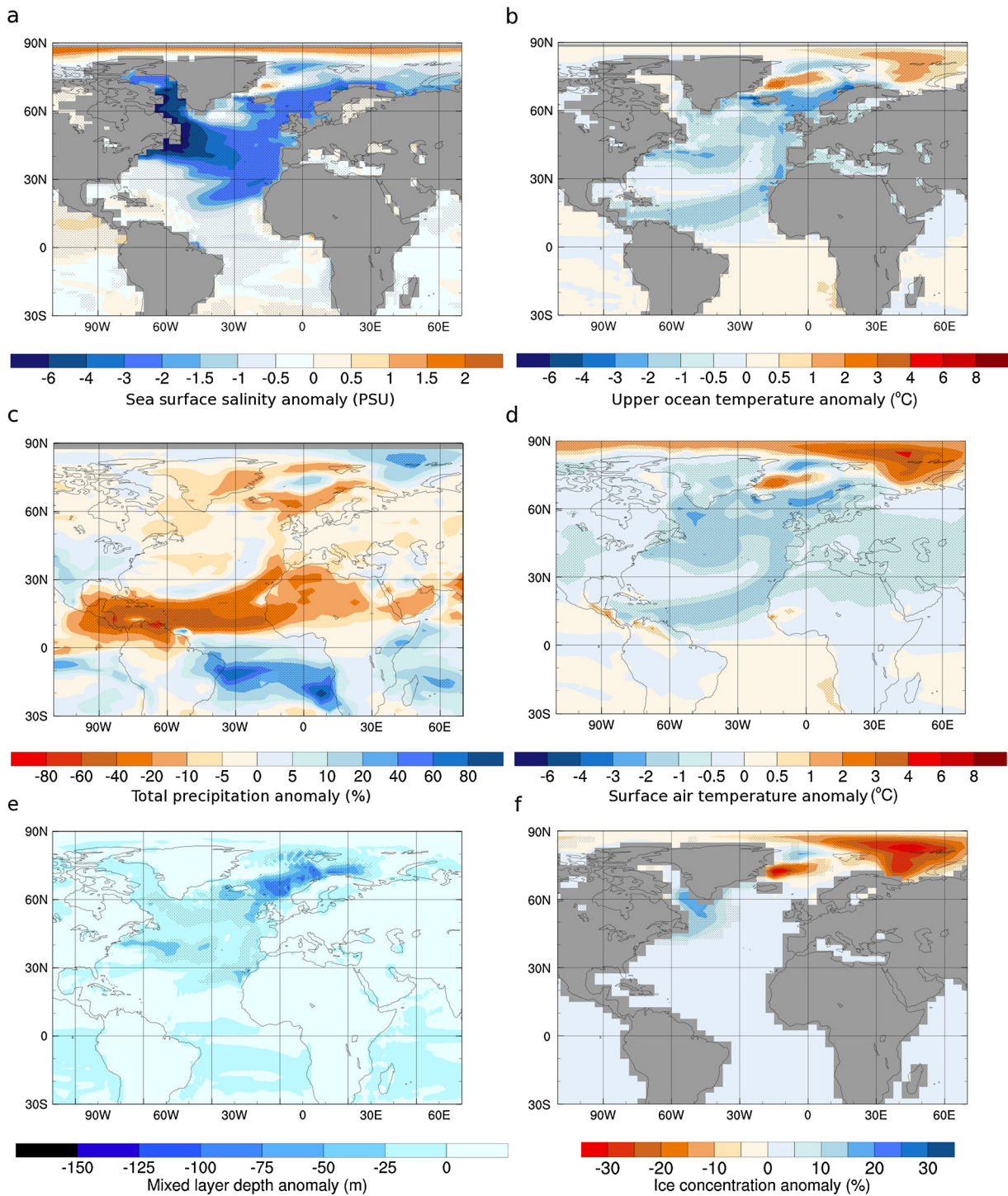


Fig. 4. Modelled climate anomalies for the 4.24m_100yr simulation with respect to the *control* run. The anomalies are calculated as annual means for a 100-yr period centred at the timing of the peak freshwater input at model year 200; (a) sea surface salinity, (b) upper ocean temperature (averaged over top 164 m), (c) precipitation, (d) surface air temperature, (e) mixed layer depth and (f) annual sea ice concentration. Stippling indicates significant difference at 99% level according to Welch's t test.

3.3. The role of duration and amplitude of meltwater pulses on the climatic response

The meltwater pulses with a magnitude of 4.24 m sea level rise (simulations 4.24m_300yr, 4.24m_200yr and 4.24m_100yr) result in changes that most closely match the observed 8.2 ka temperature changes, whereas the response to the smaller freshwater forcings in 3.62m_200yr, 3.62m_100yr is weaker and shorter (Table 2). A longer duration pulse generally results in the converse response for event duration at the proxy locations, i.e. they get

shorter. However, this is not the case for two of the marine locations closest to the forcing location (South Iceland Rise and Cape Ghir), where the longest anomalous cooling is observed in the 4.24m_300yr simulation. This is likely a result of the direct influence of the prolonged freshwater input reaching these sites and promoting the growth of sea ice, as opposed to the cooling observed in surface air temperatures over Europe and Greenland being controlled by the diminished heat transport from the tropical latitudes resulting from the weakening overturning circulation. The response in surface air temperatures further away from the forcing

location gets weaker than the event inferred from proxies as the duration of the saddle collapse is longer (e.g. difference between the event observed at Lake Røuge and Lake Arapisto in Table 2 between the 4.24m_300yr and 4.24m_100yr simulations). Both the total volume of released freshwater and the duration of the saddle collapse are important in determining the climate response, but the total volume seems to play a key role based on the similarity between the AMOC perturbation (Fig. 1b) and temperature signal (Table 2) between simulations 4.24m_200yr and 4.24m_100yr.

4. Discussion

Our simulations indicate that the freshwater input from the saddle collapse could have been the major forcing of the 8.2 ka event, but contributions of other forcings need to be considered. Hillaire-Marcel et al. (2007) suggested that topographical changes of the LIS during its demise could have contributed to the climate change during the event. This effect was evaluated in a separate manuscript that is currently under review. As shown by Ullman et al. (2016), near the ice sheet, topographical changes have a large impact, but further away the impacts are limited. The manuscript under review suggests that topography changes impact north Atlantic gyre circulation by influencing surface winds. This in turn produces sea surface temperature changes in the gyres of at most 1 °C in 500 yr around the time of the event. In Greenland and Northern Europe, the topography changes have a negligible impact on temperature. The role of ice sheet topographical changes in the 8.2 ka event is therefore of second order compared to the effect of the meltwater pulse evaluated here.

The rerouting of rivers that carry the continental runoff from precipitation–evaporation (P–E) and ice sheet meltwater from St. Lawrence River to Hudson Strait has been suggested as having been a significant forcing for the event (Clark et al., 2001; Meissner and Clark, 2006; Carlson et al., 2009b). The majority of this rerouted freshwater has been recently estimated to have originated from the LIS meltwater (Wagner et al., 2013), and that the role of the river rerouting derived from P–E was negligible. Additionally, Ivanovic et al. (2017) found that AMOC was insensitive to rerouting of ~0.05 Sv runoff from Mississippi to Hudson and St. Lawrence Rivers on centennial time scales for an earlier stage of LIS deglaciation. This is because freshwater input to western North Atlantic is rapidly mixed and dispersed by the North Atlantic gyres, so the exact point of entry to the oceans becomes less important (Ivanovic et al., 2017). In our simulations, a large fraction of the freshwater input is transported as a coastal current to where the St. Lawrence River drains to the North Atlantic before getting mixed in the subtropical gyre (Fig. 4a), making it unlikely that a change between the two locations in runoff routing had a major impact. Thus we argue that the most important factor in the 8.2 ka event is not the location of freshwater input to the western North Atlantic, but instead the temporal changes in the amount of meltwater flux entering the ocean. The opening of a new pathway for the LIS meltwater to exit through the Hudson Strait, however, likely resulted in changes in the ice sheet and a temporary increase of the FWF to the ocean, which could make the rerouting an important part of the disintegration of the Laurentide Ice Sheet.

The temporal evolution of freshwater input from the LIS to the North Atlantic was likely more complicated than represented in our simulations. The triangular forcing we used is a simplified representation of the saddle collapse meltwater pulse, but the remnant LIS likely continued to melt at an elevated rate following the collapse, as the change in albedo and enlarging area of the Hudson Bay becoming seasonally ice-free have been suggested to have accelerated the demise of the ice domes around Hudson Bay (Ullman et al., 2016). Additionally, while the impact of the lake Agassiz flood in our simulation is overridden by the impact of the sad-

dle collapse, the freshwater from Lake Agassiz could have had an amplifying effect on the signal depending on the timing of the outburst. Determining the timing of the lake release(s) with respect to the acceleration of ice melt would be crucial to evaluating this effect. Future work should investigate the combined dynamical and surface mass balance – driven ice loss using an ice sheet model capable of representing the fine-scale evolution of the ice sheet to constrain the melt and timing of the lake flood.

The temporal starting point of the simulations has also had a major effect in some studies modelling the effect of the lake outburst (e.g. LeGrande and Schmidt, 2008; Tindall and Valdes, 2011). We did not test the effect of the model weather, i.e. starting the event at different points in the ongoing background climate variability. However, multi-decadal climate variability is likely to be more important for climatic perturbations with a short forcing (1–2 yr), whereas centennial-scale forcing would dampen the dependence on the starting state. We thus reason that climate variability would have a secondary effect on the surface response to the saddle collapse meltwater pulse.

Proxy evidence from the eastern branch of the NADW overflow suggest two occurrences of reduction in surface salinity at ~8.5 ka and ~8.3 ka and a ~400 yr slowdown in deep current flow speed commencing at ~8.5 ka, which have been used as evidence for the 8.2 ka event having been a product of a two-stage freshwater forcing (Ellison et al., 2006). The first of these freshening occurrences has been thought to have preconditioned the AMOC before the second one, which would have resulted in the ~160-yr cooling signal associated with the 8.2 ka event. Interestingly, a two-stage freshening with SST minima 200 yr apart is not visible in a record from another deep-sea sediment core MD03-2665 recovered from the western branch of the NADW overflow (Kleiven et al., 2008), suggesting that the first of the freshening occurrences was not as far-reaching as the second one. The 100-yr saddle collapse of 2.85 m on top of the 0.05 Sv background flux is enough to significantly slow down the AMOC for over 200 yr in our simulation, and ice sheet modelling studies have suggested that the freshwater flux released from the ice sheet around the timing of the climate event could have been higher than in our simulations, ~5.5 m over 400 yr (Gregoire et al., 2012) and ~6.6 m over 500 yr (Carlson et al., 2008). The freshwater flux resulting from the melting ice sheet likely had a more complex structure than the linearly increasing and decreasing scenarios in our simulations (Fig. 1c), and we suggest that temporally variable LIS melt could have been responsible for producing the different phases of the event.

5. Conclusions

Based on our results and the findings of previous studies (Carlson et al., 2008, 2009a; Gregoire et al., 2012; Wagner et al., 2013), we argue that the 8.2 ka event was caused by a centennial meltwater pulse from the collapse of the Hudson Bay ice saddle in North America. The freshwater from the saddle collapse was rerouted through the Hudson Strait to the Labrador Sea (Clark et al., 2001; Carlson et al., 2009b) during the deglaciation of the Hudson Bay. This additional freshwater caused a decrease in the rate of formation of North Atlantic Deep Water, in turn resulting in a weakening of the AMOC and a reduction in meridional heat transport. With this forcing mechanism, our experiment using a GCM can reproduce the spatial pattern, duration and amplitude of this cooling event with a realistic, mechanistically-based forcing scenario.

As proposed by Gregoire et al. (2012), the outbursts of Lakes Agassiz and Ojibway (Barber et al., 1999; Teller et al., 2002) likely occurred during the collapse of the Hudson Bay ice saddle. There is general consistency between GCM studies of the 8.2 ka event that the influence of such outbursts on climate is small and short

compared to the effect of larger and longer meltwater fluxes from the Laurentide Ice Sheet (Fig. 1; LeGrande and Schmidt, 2008; Wagner et al., 2013). In climate proxy records, these smaller lake outburst perturbations may even be indistinguishable from climate variability. There is also good reason to suspect that the 8.2 ka event did not occur in two distinct stages, but was instead caused by a single, longer term forcing from ice sheet melt. This finding enables a step forward in using this event as a benchmark for climate models, as the meltwater flux from the ice sheet can be better constrained than the timing and magnitude of a more complex forcing consisting of multiple sources.

Author Contributions

ISOM, LJG and RFI designed the study. ISOM designed, performed and analysed the experiments with inputs from LJG, RFI and J.C.T. ISOM and LJG wrote the manuscript with inputs from all co-authors.

Correspondence and requests for materials should be addressed to eeisom@leeds.ac.uk.

Acknowledgements

We thank A. Carlson, T. Törnqvist and an anonymous reviewer for their helpful comments and constructive suggestions. ISOM is funded by the Leeds-York Natural Environment Research Council (NERC) Spheres Doctoral Training Partnership (NE/L002574/1). RFI is funded by NERC grant NE/K008536/1. The work made use of the N8 HPC facilities, which are provided and funded by the N8 consortium and EPSRC (EP/K000225/1) and co-ordinated by the Universities of Leeds and Manchester. Modelling support and infrastructure provided within the Faculty of Environment and Centre of Excellence for Modelling the Atmosphere and Climate (CEMAC), University of Leeds. Presented model data are available through a National Geoscience Data Centre (NGDC) repository, <http://dx.doi.org/10.5285/0c40db60-6b1e-4564-9613-95a34a2ec3d9>.

References

- Barber, D.C., Dyke, A., Hillaire-Marcel, C., Jennings, A.E., Andrews, J.T., Kerwin, M.W., Bilodeau, G., McNeely, R., Southon, J., Morehead, M.D., et al., 1999. Forcing of the cold event of 8,200 years ago by catastrophic drainage of Laurentide lakes. *Nature* 400, 344–348.
- Briggs, R.D., Tarasov, L., 2013. How to evaluate model-derived deglaciation chronologies: a case study using Antarctica. *Quat. Sci. Rev.* 63, 109–127.
- Carlson, A.E., LeGrande, A.N., Oppo, D.W., Came, R.E., Schmidt, G.A., Anslow, F.S., Licciardi, J.M., Obbink, E.A., 2008. Rapid early Holocene deglaciation of the Laurentide ice sheet. *Nat. Geosci.* 1, 620–624.
- Carlson, A.E., Anslow, F.S., Obbink, E.A., LeGrande, A.N., Ullman, D.J., Licciardi, J.M., 2009a. Surface-melt driven Laurentide ice-sheet retreat during the Early Holocene. *Geophys. Res. Lett.* 36. <http://dx.doi.org/10.1029/2009GL040948>.
- Carlson, A.E., Clark, P.U., Haley, B.A., Klinkhammer, G.P., 2009b. Routing of western Canadian Plains runoff during the 8.2 ka cold event. *Geophys. Res. Lett.* 36. <http://dx.doi.org/10.1029/2009GL038778>.
- Clark, P.U., Marshall, S.J., Clarke, G.K.C., Hostetler, S.W., Licciardi, J.M., Teller, J.T., 2001. Freshwater forcing of abrupt climate change during the last glaciation. *Science* 293, 283–287.
- Clarke, G.K.C., Leverington, D.W., Teller, J.T., Dyke, A.S., 2004. Paleohydraulics of the last outburst flood from glacial Lake Agassiz and the 8200 BP cold event. *Quat. Sci. Rev.* 23, 389–407.
- Condron, A., Winsor, P., 2011. A subtropical fate awaited freshwater discharged from glacial Lake Agassiz. *Geophys. Res. Lett.* 38, L03705.
- Dyke, A.S., Prest, V.K., 1987. Late Wisconsinan and Holocene history of the Laurentide Ice Sheet. *Geogr. Phys. Quat.* 41, 237.
- Ellison, C.R.W., Chapman, M.R., Hall, I.R., 2006. Surface and deep ocean interactions during the cold climate event 8200 years ago. *Science* 312, 1929–1932.
- Feurdean, A., Klotz, S., Moosbrugger, V., Wohlfarth, B., 2008. Pollen-based quantitative reconstruction of Holocene climate variability in NW Romania. *Palaeogeogr. Palaeoclimatol. Palaeoecol.* 260, 494–504.
- Grafenstein, U., von Erlenkeuser, H., Müller, J., Jouzel, J., Johnsen, S., 1998. The cold event 8200 years ago documented in oxygen isotope records of precipitation in Europe and Greenland. *Clim. Dyn.* 14, 73–81.
- Gregoire, L.J., Payne, A.J., Valdes, P.J., 2012. Deglacial rapid sea level rises caused by ice-sheet saddle collapses. *Nature* 487, 219–222.
- Gregoire, L.J., Valdes, P.J., Payne, A.J., 2015. The relative contribution of orbital forcing and greenhouse gases to the North American deglaciation. *Geophys. Res. Lett.* 42, 2015GL066005.
- Hillaire-Marcel, C., de Vernal, A., Piper, D.J.W., 2007. Lake Agassiz Final drainage event in the northwest North Atlantic. *Geophys. Res. Lett.* 34, L15601. <http://dx.doi.org/10.1029/2007GL030396>.
- Hoffman, J.S., Carlson, A.E., Winsor, K., Klinkhammer, G.P., LeGrande, A.N., Andrews, J.T., Strasser, J.C., 2012. Linking the 8.2 ka event and its freshwater forcing in the Labrador Sea. *Geophys. Res. Lett.* 39, L18703.
- Ivanovic, R.F., Gregoire, L.J., Wickert, A.D., Valdes, P.J., Burke, A., 2017. Collapse of the North American ice saddle 14,500 years ago caused widespread cooling and reduced ocean overturning circulation. *Geophys. Res. Lett.* 44, 2016GL071849.
- Kim, J.-H., Meggers, H., Rambu, N., Lohmann, G., Freudenthal, T., Müller, P.J., Schneider, R.R., 2007. Impacts of the North Atlantic gyre circulation on Holocene climate off northwest Africa. *Geology* 35, 387–390.
- Kleiven, H. (Kikki) F., Kissel, C., Laj, C., Ninnemann, U.S., Richter, T.O., Cortijo, E., 2008. Reduced North Atlantic deep water coeval with the glacial Lake Agassiz freshwater outburst. *Science* 319, 60–64. <http://dx.doi.org/10.1126/science.1148924>.
- Kobashi, T., Severinghaus, J.P., Brook, E.J., Barnola, J.-M., Grachev, A.M., 2007. Precise timing and characterization of abrupt climate change 8200 years ago from air trapped in polar ice. *Quat. Sci. Rev.* 26, 1212–1222.
- Lambeck, K., Rouby, H., Purcell, A., Sun, Y., Sambridge, M., 2014. Sea level and global ice volumes from the Last Glacial Maximum to the Holocene. *Proc. Natl. Acad. Sci.* 111, 15296–15303.
- LeGrande, A.N., Schmidt, G.A., 2008. Ensemble, water isotope-enabled, coupled general circulation modeling insights into the 8.2 ka event. *Paleoceanography* 23, PA3207.
- Leverington, D.W., Mann, J.D., Teller, J.T., 2002. Changes in the bathymetry and volume of glacial Lake Agassiz between 9200 and 7700 14C yr B.P. *Quat. Res.* 57, 244–252.
- Lewis, C.F.M., Miller, A.A.L., Levac, E., Piper, D.J.W., Sonnichsen, G.V., 2012. Lake Agassiz outburst age and routing by Labrador Current and the 8.2 cal ka cold event. *Quat. Int.* 260, 83–97.
- Li, Y.-X., Törnqvist, T.E., Nevitt, J.M., Kohl, B., 2012. Synchronizing a sea-level jump, final Lake Agassiz drainage, and abrupt cooling 8200 years ago. *Earth Planet. Sci. Lett.* 315–316, 41–50.
- Licciardi, J.M., Teller, J.T., Clark, P.U., 1999. Freshwater routing by the Laurentide Ice Sheet during the last deglaciation. In: Clark, P.U., Webb, R.S., Keigwin, L.D. (Eds.), *Mechanisms of Global Climate Change at Millennial Time Scales*. American Geophysical Union, pp. 177–201.
- LoDico, J.M., Flower, B.P., Quinn, T.M., 2006. Subcentennial-scale climatic and hydrologic variability in the Gulf of Mexico during the early Holocene. *Paleoceanography* 21, PA3015.
- Meissner, K.J., Clark, P.U., 2006. Impact of floods versus routing events on the thermohaline circulation. *Geophys. Res. Lett.* 33, L15704.
- Morrill, C., Anderson, D.M., Bauer, B.A., Buckner, R., Gille, E.P., Gross, W.S., Hartman, M., Shah, A., 2013a. Proxy benchmarks for intercomparison of 8.2 ka simulations. *Clim. Past* 9, 423–432.
- Morrill, C., LeGrande, A.N., Renssen, H., Bakker, P., Otto-Bliesner, B.L., 2013b. Model sensitivity to North Atlantic freshwater forcing at 8.2 ka. *Clim. Past* 9, 955–968.
- Mortyn, P.G., Charles, C.D., 2003. Planktonic foraminiferal depth habitat and $\delta^{18}\text{O}$ calibrations: plankton tow results from the Atlantic sector of the Southern Ocean. *Paleoceanography* 18, 1037.
- Peltier, W.R., 2004. Global glacial isostasy and the surface of the Ice-age Earth: the ICE-5G (VM2) Model and GRACE. *Annu. Rev. Earth Planet. Sci.* 32, 111–149.
- Renssen, H., Goosse, H., Fichefet, T., Campin, J.-M., 2001. The 8.2 kyr BP event simulated by a global atmosphere–sea–ice–ocean model. *Geophys. Res. Lett.* 28, 1567–1570.
- Rohling, E.J., Pälike, H., 2005. Centennial-scale climate cooling with a sudden cold event around 8,200 years ago. *Nature* 434, 975–979.
- Sarmaja-Korjonen, K., Seppä, H., 2007. Abrupt and consistent responses of aquatic and terrestrial ecosystems to the 8200 cal. yr cold event: a lacustrine record from Lake Arapisto, Finland. *Holocene* 17, 457–467.
- Schmidt, G.A., LeGrande, A.N., 2005. The Goldilocks abrupt climate change event. *Quat. Sci. Rev.* 24, 1109–1110.
- Singarayer, J.S., Valdes, P.J., Friedlingstein, P., Nelson, S., Beerling, D.J., 2011. Late Holocene methane rise caused by orbitally controlled increase in tropical sources. *Nature* 470, 82–85.
- Stouffer, R.J., Yin, J., Gregory, J.M., Dixon, K.W., Spelman, M.J., Hurlin, W., Weaver, A.J., Eby, M., Flato, G.M., Hasumi, H., et al., 2006. Investigating the causes of the response of the thermohaline circulation to past and future climate changes. *J. Climate* 19, 1365–1387.
- Teller, J.T., Leverington, D.W., Mann, J.D., 2002. Freshwater outbursts to the oceans from glacial Lake Agassiz and their role in climate change during the last deglaciation. *Quat. Sci. Rev.* 21, 879–887.
- Thomas, E.R., Wolff, E.W., Mulvaney, R., Steffensen, J.P., Johnsen, S.J., Arrowsmith, C., White, J.W.C., Vaughn, B., Popp, T., 2007. The 8.2 ka event from Greenland ice cores. *Quat. Sci. Rev.* 26, 70–81.

- Thornalley, D.J.R., Elderfield, H., McCave, I.N., 2009. Holocene oscillations in temperature and salinity of the surface subpolar North Atlantic. *Nature* 457, 711–714.
- Tindall, J.C., Valdes, P.J., 2011. Modeling the 8.2 ka event using a coupled atmosphere–ocean GCM. *Glob. Planet. Change* 79, 312–321.
- Törnqvist, T.E., Hijma, M.P., 2012. Links between early Holocene ice-sheet decay, sea-level rise and abrupt climate change. *Nat. Geosci.* 5, 601–606.
- Ullman, D.J., Carlson, A.E., Hostetler, S.W., Clark, P.U., Cuzzone, J., Milne, G.A., Winsor, K., Caffee, M., 2016. Final Laurentide ice-sheet deglaciation and Holocene climate–sea level change. *Quat. Sci. Rev.* 152, 49–59.
- Valdes, P.J., Armstrong, E., Badger, M.P.S., Bradshaw, C.D., Bragg, F., Davies-Barnard, T., Day, J.J., Farnsworth, A., Hopcroft, P.O., Kennedy, A.T., et al., 2017. The BRIDGE HadCM3 family of climate models: HadCM3@Bristol v1.0. *Geosci. Model Dev. Discuss.* 2017, 1–42.
- Veski, S., Seppä, H., Ojala, A.E.K., 2004. Cold event at 8200 yr B.P. recorded in annually laminated lake sediments in eastern Europe. *Geology* 32, 681–684.
- Wagner, A.J., Morrill, C., Otto-Bliesner, B.L., Rosenbloom, N., Watkins, K.R., 2013. Model support for forcing of the 8.2 ka event by meltwater from the Hudson Bay ice dome. *Clim. Dyn.* 41, 2855–2873.
- Weldeab, S., Lea, D.W., Schneider, R.R., Andersen, N., 2007. Centennial scale climate instabilities in a wet early Holocene West African monsoon. *Geophys. Res. Lett.* 34, L24702.
- Wiersma, A.P., Jongma, J.I., 2010. A role for icebergs in the 8.2 ka climate event. *Clim. Dyn.* 35, 535–549.
- Wiersma, A.P., Renssen, H., Goosse, H., Fichefet, T., 2006. Evaluation of different freshwater forcing scenarios for the 8.2 ka BP event in a coupled climate model. *Clim. Dyn.* 27, 831–849.